Application of Voronoi Tessellation for Modeling Randomly Packed Hollow-Fiber Bundles

Vicki Chen and Marc Hlavacek
Centre for Membrane Science and Technology, School of Chemical Engineering and Industrial Chemistry, University of New South Wales, Kensington, New South Wales 2033, Australia

Influence of local voids on flow maldistribution in randomly packed fiber bundles is examined by Voronoi tessellation. A theoretical expression for the local void distribution caused by random placement of fibers is developed by using a random-cell model. Simulations and packing experiments have been conducted to assess the accuracy of the theoretical distribution of cell sizes. In the case of shell side, laminar flow parallel to the fibers, the theoretical distribution is used to estimate fRe (friction factor times Reynolds number) and volumetric flows, and to compare results with ordered arrays and experimental data from literature. The results are used to assess the contributions of local voidage variations to flow bypass. This has implications for the prediction of pressure drop and heat and mass transfer in hollow-fiber module applications where transport is dominated by flow on the shell side.

Introduction

Hollow-fiber modules consisting of fiber bundles in a tube and shell configuration have been used in many applications such as filtration or contactor devices. They are being studied for use in membrane distillation and other separation processes. Recent applications also include bioreactors. Mass transfer, heat transfer, and fluid dynamics in these modules have been extensively studied, assuming that the fibers are placed in ordered arrays (Shah and London, 1978; Wickramasinghe et al., 1991, 1992). However, the fibers, often numbering in the hundreds in a single bundle, are usually randomly packed in the module. There exists little literature on the effect of random-fiber replacement on the performance of the modules, except in general acknowledgment of its possible role in fluid bypass (Noda et al., 1979).

In many hollow-fiber module applications, reduction of mass- and heat-transfer efficiency occurs due to the bypass of fluid around large numbers of fibers. This effect, also known as channeling, has a variety of causes such as irregular flow areas, fiber movement during operation, and the positioning of inlets and outlets. Recent studies suggested that twisting or winding of fibers may be a way to reduce observed channeling (Wickramasinghe et al., 1991, 1992). One possible contributor to channeling is the local variation of fiber spacing due to random-fiber placement during the potting procedure used for fiber bundle assembly.

Although the fibers are randomly packed in the modules, many studies of hollow-fiber module operations assume ordered packing. This is done because of the ease of calculations due to the symmetry of the flow fields (Happel, 1959; Sparrow and Loeffler, 1959) and the enormous amount of experimental data in the literature available from heat-transfer studies using ordered tube banks (Shah and London, 1978). Theoretical solutions for the skin drag component of the pressure drop have been provided over the entire range of packing densities (Sparrow, 1959). However, for randomly packed bundles, exact solutions for every fiber are not practical. Experimental results at intermediate packing densities show that pressure drops and residence time tracer analyses deviate significantly from calculations for ordered arrays (Yang and Cussler, 1986; Noda et al., 1979). At very high random packing densities (around 80%), locally ordered arrays begin to appear. In contrast, at low packing densities, the flow around each fiber becomes independent of neighboring fibers. Unlike heat exchangers, commercially available hollow-fiber modules often have large numbers of fibers and are randomly packed at intermediate packing densities (around 50%). These conditions are chosen for ease of assembly, economic considerations, and pressure drop considerations. Modeling of intermediate pack-

Correspondence concerning this article should be addressed to V. Chen.

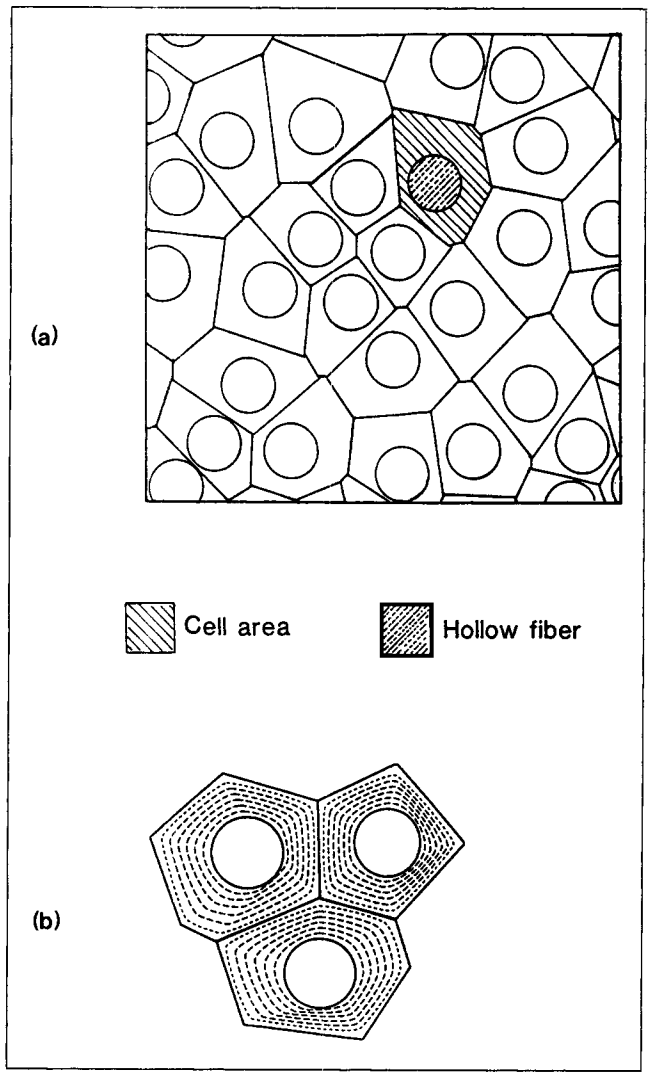

Figure 1. (a) Voronoi tessellation of flow area; (b) schematic of velocity contours between fibers defined by tessellation cells.

ing densities is thus an important consideration in the design and operation of hollow-fiber modules.

A few studies have considered the effect of random-fiber placement on flow perpendicular to the cylinders (Kuwabra, 1959) and across fibrous filters (Yu and Soong, 1975). For flow parallel to the fiber, pressure drops have been experimentally determined by Sullivan (1942) for compact bundles of small diameter, solid fibers. Costello et al. (1993) have examined the effect of nonuniform packing on pressure drop and mass transfer for small microfiltration hollow fibers. Other studies have examined the effect of flow maldistribution experimentally from the difference between expected and actual mass-transfer performance. The total contribution of channeling from all sources has been examined as a function of packing density by studying various fiber orientations, NMR flow imaging and tracer residence time distribution (Noda et al., 1979; Yang and Cussler, 1986; Wickramasinghe et al., 1991; Wickramasinghe et al., 1992; Heath et al., 1990; Hammer et al., 1990).

This article describes the use of Voronoi tessellations to model fiber placements and its contribution to channeling in randomly packed bundles. Voronoi tessellation is a method to describe the subdivision of space between randomly packed objects by drawing straight boundaries equidistant between neighboring objects, forming polygonal cells. Voronoi tessellation is an attractive technique to analyze randomly packed fiber modules because it provides a way to calculate the geometric characteristics of random spacing that can be used to calculate overall properties.

In this article, each fiber is considered to be surrounded by a polygonal cell defined by a Voronoi tessellation, described in detail below. The distribution of voidage and geometric characteristics of each cell reflect the effect of random placement of neighboring fibers. The effects of such local variation of voidage on flow distribution, pressure drop, heat and mass transfer have previously been estimated for packed beds of spherical particles by Haughey and Beveridge (1966, 1967) using effective hydraulic diameters. Using this approach, the distribution of cell sizes is used to calculate the distribution of voidages around the fibers. The change in the effective friction factor times the Reynolds number (fRe) is then calculated as a measure of the effect of channeling on pressure drop. Applications to the calculation of other variables such as mass-transfer and heat-transfer coefficients are outlined.

Modeling of Randomly Packed Hollow Fibers

Voronoi tesselation

Fiber bundles are regarded as a collection of parallel, rigid rods as shown in Figure 1a. The random packing of these rods may be simulated by the packing of monodispersed disks in a two-dimensional cross section of the fiber module (Tomadakis and Sotirchos, 1991). A range of techniques exist for generating two-dimensional packing geometries, and these have been used to simulate fiber bundles.

In order to assess the effect of random-fiber placement, the cross-sectional area of the module is subdivided into smaller areas associated with each fiber. Each fiber is surrounded by a polygonal cell whose boundaries are defined by perpendicular bisectors of lines joining each fiber with its nearest neighbor. A typical Voronoi polygon is shown in Figure 1a. The distribution of polygon areas can then be determined for any given geometry, and this in turn gives the local porosity distribution. Such a geometrical approach has been extensively used in modeling porous media, including membranes (Chan et al., 1990).

Flow through the fiber module is complicated by the irregularity of the voids, making it difficult to determine detailed velocity profiles. At the boundaries of the Voronoi polygons, the velocity is at a maximum as they are equidistant from the adjacent fibers. A schematic of the velocity contours in adjacent fibers is shown in Figure 1b.

The simplest means to generate a cross section of non-overlapping, randomly placed fibers is to implement a random sequential addition (RSA) scheme where disks (fibers cross-sections) are randomly placed with the restriction of no overlap. Although this method has been used to study the availability of circular voids in 2D packing of disks, it is not capable of consistently producing packing densities greater than 55% (Alonso et al., 1992; Hinrichsen et al., 1986). Other simulation methods, such as the Metropolis Monte Carlo technique, can be used to generate higher packing densities. Glaser and Clark (1993) used a Voronoi tessellation of simulated high random

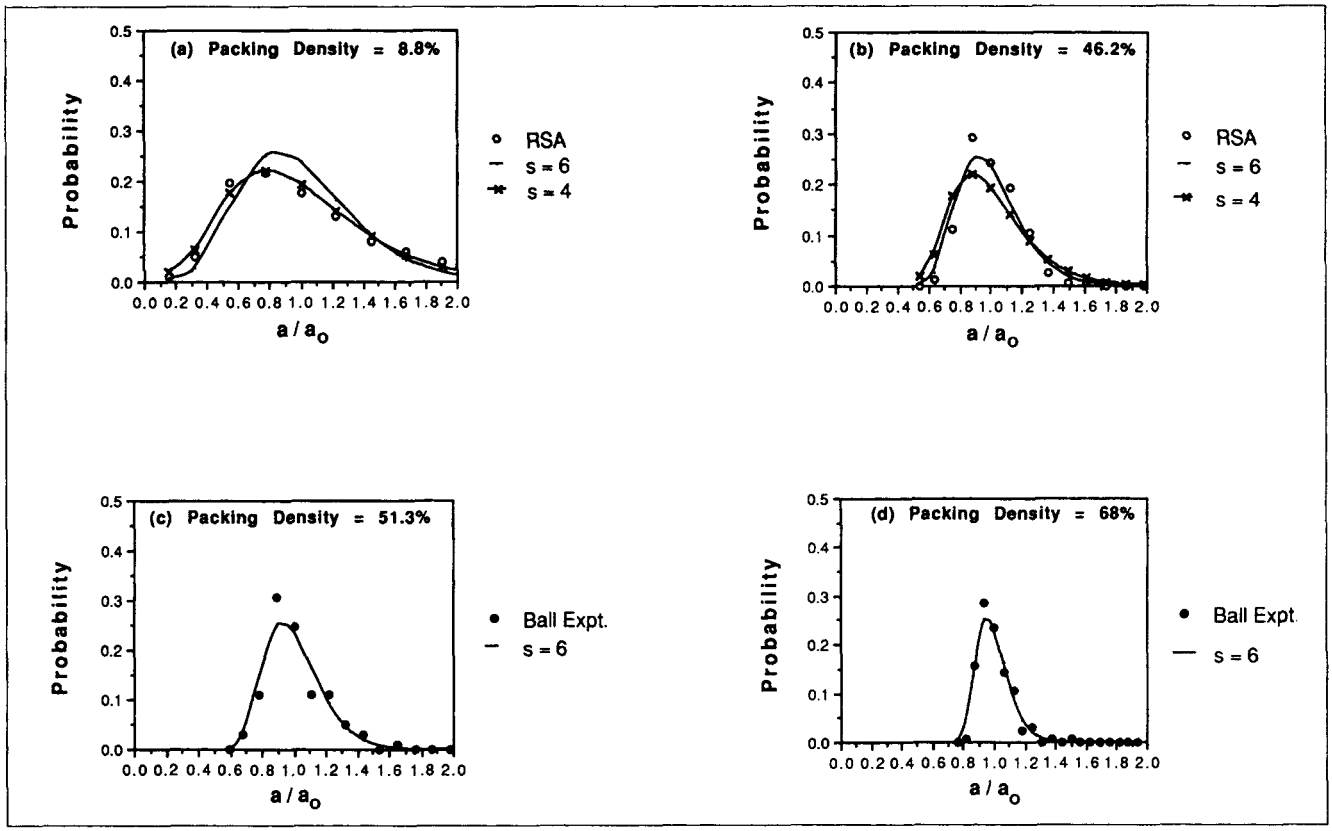

Figure 2. (a), (b), Calculated and simulated (RSA) probability of cell sizes plotted as a function of a/a_o; (c), (d) calculated and experimental (using steel balls) probability of cells sizes plotted as a function of a/a_o.

packing densities (0.7 to 0.91) to examine cell size distributions and determine the contributions of ordered and disordered regions in the melting of 2D crystal structures. This article considers a theoretical method to estimate the area distribution over the entire range of packing densities and compares the results to simulations using RSA and packing experiments using randomly positioned steel balls.

Probability density function

Consider N fibers which are randomly placed in an area, A, which is the cross-sectional area of a module. The probability that there is no other fiber within an area ϕ is described by an exponential probability density function:

$$f(\phi)=\frac{1}{\langle\phi\rangle}\,e^{-(\phi)/\langle\phi\rangle}, \tag{1}$$

which fulfills the criteria that:

$$\int_{\phi_{\min}}^{\phi_{\max}}\phi f(\phi)d\phi=\langle\phi\rangle \text{ and } \int_{\phi_{\min}}^{\phi_{\max}} f(\phi)d\phi=1 \tag{2}$$

where $\langle\phi\rangle$ is the average area per fiber. However, as one can see in Figure 2a, the area associated with each fiber in the Voronoi tessellation is determined not just by the location of the nearest neighbor but by the location of all the nearest neighbors surrounding the fiber. This ranges from an average of four (at low packing densities) to six (at the limit of hexagonal close packing).

Thus, the area per fiber is actually a composite of randomly but identically distributed areas determined by the fiber's nearest neighbors. Chan et al. (1988) have solved this composite probability density function comprising s separate exponential distributions:

$$f(\phi)=\frac{s^s}{\langle\phi\rangle^s}\,\frac{\phi^{s-1}}{(s-1)!}\,e^{-s\phi/\langle\phi\rangle} \tag{3}$$

In this context, s is the number of nearest neighbors, and the distribution of areas can be determined directly by integrating the probability density function.

Before comparison between the calculated and simulated results can be done, the finite size of the fiber must be taken into account since an increase in packing density will decrease the amount of "free" area that neighboring fibers can occupy. One way to account for this has been described by Frenkel (1955). The loss of "free" area is taken into consideration by substituting:

$$a-a_f=\phi \text{ and } a_o-a_f=\langle\phi\rangle \tag{4}$$

where a is the cross-sectional area of a cell containing a particular fiber (including the fiber), a_o is the average cross-sectional area per fiber (including the area of the fiber), and a_f is the minimum cross-sectional area that a fiber can occupy. For a fiber with a circular cross section with a radius r:

$$a_f = 1.1207\ \pi r^2 \tag{5a}$$

for a fiber circumscribed by a hexagon for a triangular array and

$$a_f = 1.2732\ \pi r^2 \tag{5b}$$

for a fiber circumscribed by a square for a square array. Thus, when $s = 6$, the probability density function can be written as:

$$f(\phi) = \frac{6^6}{a_o - a_f}\frac{\lambda^5}{5!}e^{-6\lambda} \tag{6}$$

where

$$\lambda = \frac{(a - a_f)}{(a_o - a_f)} \tag{7}$$

and the probability of a cell having an area between a_1 and a_2 is:

$$P = \int_{\lambda_1}^{\lambda_2} 6^6 \frac{\lambda^5}{5!} e^{-6\lambda} d\lambda. \tag{8}$$

where

$$\lambda_1 = \frac{(a_1 - a_f)}{(a_o - a_f)} \text{ and } \lambda_2 = \frac{(a_2 - a_f)}{(a_o - a_f)}$$

and similarly for $s = 4$.

Comparison between simulation, packing experiments and probability density function

Simulation using random sequential addition followed by Voronoi tessellation was carried out allowing no overlap of fibers to check the effectiveness of the probability density equations. The areas generated by the simulation were then tabulated according to size. This was done for packing densities from 6% to 47% and then compared with the calculated probability using more than 100 points for each packing density for $s = 4$ and 6.

Figure 2a and 2b shows probability plotted against area normalized with respect to average cell area. At lower packing densities, $s = 4$ appears to fit the simulation better, as predicted by Meijering (1953). At higher packing densities, the calculated distribution agrees better with $s = 6$. This is expected as there are six nearest neighbors in the limit of close packing. To measure the area distribution at higher packing densities than achievable by RSA, cell size distributions were generated using randomly positioned steel balls which can move freely. Experiments were conducted at packing densities of 51% to 68%. One layer of steel balls [3.2×10^{-3} m (0.125 in.) diameter from Australian Ball Co.] was packed in a hexagonal cell mounted on a speaker driven at 70 Hz. The positions of the balls were randomized by the variations of the speaker. The balls' positions were captured by a charge capture device (CCD) array video camera (TCG Systems Automation, Pty. Ltd., Chippendale, Australia) and stored on computer using a Video Blaster frame grabber card (Creative Labs, 1901 McCarthy Blvd., Milpitas, CA). Particle coordinates were then determined using Global Labs image analysis software (Data Translation Inc., 100 Locke Drive, Marlboro MA). Voronoi tessellation of the ball positions allowed cell area distributions to be determined at high packing densities (Figures 2c and 2d). The area distributions from the steel ball experiments and the RSA simulations agreed with each other. The results of Glaser and Clark (1993) and Hinrichsen et al. (1986) using computer simulation also gave similar area distributions to the packing experiments.

The results show that the probability distribution is an asymmetric curve with a tail at high cell sizes. As the packing density increases, the shape of the curve becomes narrower and more symmetric about $a/a_o = 1$. The probability density function follows the shape changes of the curve very well and gives a reasonable estimate of the geometric characteristics of the areas surrounding the fiber and local variations of voidage. Using $s = 6$, the maximum peak height at higher packing densities is consistently underestimated, which suggests that area distribution becomes correlated to more than an average of six nearest neighbors. This is probably due to longer range correlations coming into effect which requires acknowledgment of the influence of disk packing further away than the nearest neighbors. In general, however, the calculated distribution provides a very good estimate of the cell sizes.

Effect of Random Packing on Flow Distribution in Rigid Fiber Modules

Membrane modules are often run in the laminar flow regime with flow parallel to the fibers. In the case of fully developed laminar flow parallel to the fibers on the shell side, the effect of the area distributions on pressure drop along the module can be calculated from methods used for treating heat-transfer rod bundles. Since the cell geometries are irregular, one way to estimate the effect of uneven fiber spacing is to approximate the local flow in the cells as corresponding to that of an equivalent ordered array of the same local porosity and number of neighbors. This calculation for the effective friction factor (f) times Reynolds number ($Re = D_h v\rho/\nu$) is analogous to the treatment by Shah and London (1978) and Rehme (1971) for heat exchangers which have varying local flow distributions due to the presence of walls and corners in a rod bundle. This technique estimates overall effective fRe for rod bundles from local fRes by dividing the bundle into regions of different geometries (Rehme, 1971) and treating them as separate flow areas. Using the assumptions that the entrance and exit losses are small and that flow areas are parallel and of the same length L, the pressure drop (Δp) for laminar flow through each of the separate flow areas is the same and is given by:

$$\Delta p = \frac{4L\rho v_i^2}{D_{hi}} = \left(\frac{2\nu L}{\rho}\right)\left(\frac{(fRe)_i}{A_{ci}D_{hi}^2}\right)Q_i \tag{9a}$$

where ρ is the fluid density, ν is the fluid viscosity, D_h is the hydraulic diameter, v is the velocity, A_c is the cross-sectional area for flow, Q is the fluid flow rate, and the subscript i indicate the value for the ith flow area. Over the whole bundle of N flow areas, the pressure drop is also given by Shah and London (1978):

$$\Delta p = \left(\frac{2\nu L}{\rho}\right)\left(\frac{(fRe)_e}{A_c D_h^2}\right) Q \tag{9b}$$

where

$$A_c = \sum_{i=1}^{N} A_{ci} \tag{9c}$$

$$P_w = \sum_{i=1}^{N} P_{wi} \tag{9d}$$

$$D_h = \frac{4A_c}{P_w} \tag{9e}$$

$$Q = \sum_{i=1}^{N} Q_i \tag{9f}$$

given that D_h is the hydraulic diameter, P_w represents total wetted perimeter, A_c is total cross-sectional area for flow, and Q is total fluid flow rate. Since Δp is the same for each separate flow area and across the whole bundle, Eqs. 9a and 9b can be substituted into Eq. 9f to give the effective value of fRe:

$$\frac{1}{(fRe)_e} = \sum_{i=1}^{N} \frac{1}{(fRe_i)} \left(\frac{D_h}{D_{hi}}\right)^2 \left(\frac{A_{ci}}{A_c}\right) \tag{9g}$$

where $(fRe)_e$ is the effective fRe for the overall bundle. Substituting Eq. 9e into Eq. 9f yields:

$$\frac{1}{(fRe)_e} = \sum_{i=1}^{N} \frac{1}{(fRe_i)} \left(\frac{P_w}{P_{wi}}\right)^2 \left(\frac{A_{ci}}{A_c}\right)^3 \tag{9h}$$

where P_{wi} is the wetted perimeter of the ith cell, A_c is the cross-sectional area available for flow, and A_{ci} is the flow area of the ith cell. In practice, a histogram describing the area distribution may be constructed consisting of m categories. Each category represents a size interval of the area distribution. The effective fRe is then given by:

$$\frac{1}{(fRe)_e} = \sum_{i=1}^{m} \frac{1}{(fRe_i)} N_i \left(\frac{P_w}{P_{wi}}\right)^2 \left(\frac{A_{ci}}{A_c}\right)^3 \tag{10}$$

where N_i is the number of cells in the ith category. By dividing a heat exchanger rod bundle into channels defined by where the velocity gradient was considered zero (analogous to Voronoi tessellation), Rehme (1971) used Eq. 10 to superimpose the solutions to local fRes to calculate overall fRe of a heat exchanger rod bundle, achieving very good results when compared to detailed numerical analysis of the bundles.

Applying the same method to the fiber bundle, the value of $(fRe)_i$ was determined by selecting the fRe with the same porosity from the fRe data for ordered arrays. If each Voronoi tessellation cell is considered as a separate channel using this approach, the wetted perimeter is $2\pi r$ (total wetted perimeter is $\approx N2\pi r$); the cross-sectional area for flow is given by $a_i - \pi r^2$ for each channel (total wetted channel $= A - N\pi r^2$), and the probability of each channel occurring is $P_i = N_i/N$. Equation 10 can then be rewritten as:

$$\frac{1}{(fRe)_e} = \sum_{i=1}^{m} \frac{1}{(fRe)_i} N^2 \left(\frac{a_i - \pi r^2}{A - N\pi r^2}\right)^3 N_i = \sum_{i=1}^{m} \frac{1}{(fRe)_i} \left(\frac{a_i/a_o - (1-\epsilon)}{\epsilon}\right)^3 P_i \tag{11}$$

where $(fRe)_e$ is the effective fRe for the fiber bundle, $A - N\pi r^2 = A\epsilon$, and $\epsilon = 1 - (\pi r^2/a_o)$ is the mean (bulk) porosity. The calculations shown in Figure 3 used $m = 13$ and includes over 99.9% of the cell size distribution. Little effect on $(fRe)_e$ was seen when size intervals were halved, doubling m to 26 categories.

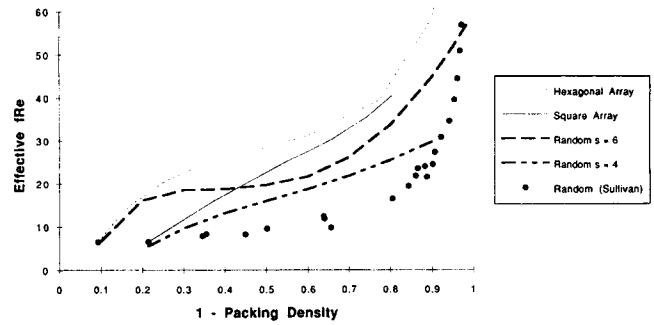

Figure 3. $(fRe)_e$ for ordered arrays (Shah et al., 1978), randomly packed fibers calculated using $s = 4$ or 6, and randomly packed textile fibers (Sullivan, 1942).

Figure 3 shows a comparison of $(fRe)_e$ calculated from Eq. 11 for random packing of fibers with experimental values obtained by Sullivan for randomly packed textile and other fibers, and with values for ordered arrays (Shah and London, 1978). Although the actual cells can have different numbers of neighbors, the two curves of $(fRe)_e$ shown in Figure 3 use values of four and six neighbors, with data for square and triangular arrays used to determine local $(fRe)_i$ for $s = 4$ and $s = 6$, respectively. The curve for random packing and $s = 6$ should be compared with the hexagonal array (Shah and London, 1978), while the randomly packed model for $s = 4$ should be compared with the square array (Shah and London, 1978). In both cases,

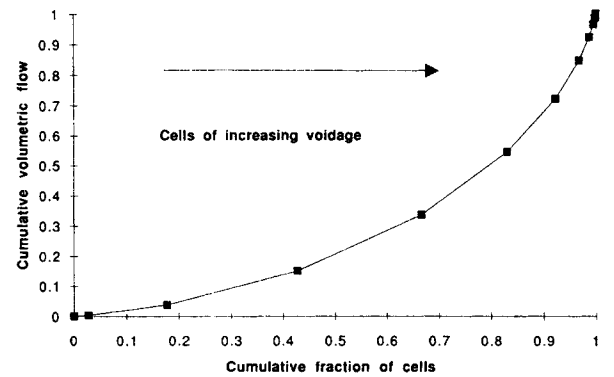

Figure 4. Cumulative flow as a function of cumulative fraction of cells.

it can be seen that the effect of random packing is to depress the value of $(fRe)_e$.

The reduction in $(fRe)_e$ is also consistent with the experimental results shown by Sullivan (1942). The Sullivan (1942) data shows greater decrease in $(fRe)_e$, but that can be due to the fact that fine fibers were used. Fiber movement during pressure drop experiments is more likely with these small fibers than more rigid fibers, causing a lower $(fRe)_e$. At low packing densities (high porosities), the effect of neighboring fibers should decrease; however, the curves for $s=4$ and $s=6$ do not converge at low packing densities. The discrepancy could be due to the fact that the weighting term $((a_i/a_o-(1-\epsilon))/\epsilon)^3$ in Eq. 11 blows up near $\epsilon \approx 1$, making the equation very sensitive to small calculation errors. Subdivision of the flow around each fiber is also no longer realistic at very high porosities since the effect of neighboring fibers is negligible, and wall effects also become significant. At high packing densities, the fRe calculated for random packing converges smoothly into the results for ordered array near the 80% packing density. Modules approaching this high packing density begin to show local ordering of fibers, and the fRe reflects this.

The fractional flow through each channel can be calculated by an equation similar to that given by Shah and London (1978):

$$W_i = P_i\left(\frac{(fRe)_e}{(fRe)_i}\right)\left(\frac{a_i/a_o-(1-\epsilon)}{\epsilon}\right)^3 \qquad (12)$$

where W_i is the fractional flow through the ith channels. For $\epsilon=0.5$, Figure 4 shows the cumulative flow compared to the cumulative fraction of cells. As expected from the area distribution, a significant amount of flow occurs through a small number of large voids. Cells in the largest 20% of the total number of cells carry 50% of the flow.

Discussion and Conclusions

The results obtained show that the geometric characteristics of randomly packed hollow fiber molecules can be calculated using Voronoi tessellation methods and a simple probability density function. Voidage variations caused by the random placement have been successfully determined. Using a crude model to assess the impact of the voidage variation on pressure drop, a significant reduction in the pressure drop can be accounted for by the flow maldistribution caused by channeling through the randomly distributed gaps.

Since rigid fibers were assumed, this model does not account for the effect of fiber movement. This can occur when hollow fibers swell or are assembled loosely within the module, resulting in clumping or bending of fibers and large gaps during fluid flow (Costello et al., 1993; Yang and Cussler, 1986). When the flow is not parallel to the fiber axis (due to bent or loose fibers or if fibers are deliberately twisted to improve mass transfer), form (inertial) drag must also be added in calculating expected pressure drops and transport properties. Even when more complex secondary flows are used to describe fluid flow and mass transfer in these bundles, the application of Voronoi tessellation to visualize and analyze module cross-sections can still yield the distribution of fiber spacings and estimate theoretical flow distributions.

Using the fiber spacing distribution, average mass- and heat-transfer coefficients can also be calculated for flow in these hollow fiber modules. Using a Gaussian distribution of fiber sizes, Wickramasinghe et al. (1992) recently calculated the effect of variation of lumen flow areas on the mass-transfer coefficient. With the fiber spacing distribution calculated here, it is possible to use the same technique suggested by Wickramasinghe et al. (1992) to calculate mass-transfer coefficients for the flows parallel to and outside the fibers, accounting for random fiber packing. Treating the fiber bundle as a distribution of cell sizes, it is also possible to calculate heat-transfer coefficients using the techniques outlined by Shah and London (1978) for parallel multigeometry passages. The impact of random packing will vary widely with configuration of heat exchangers and contactors (Shah and London, 1978). Random packing is likely to have a significant effect in predicting the theoretical flows and efficiencies of heat and mass transfer for hollow fiber units in membrane distillation and bioreactors, depending on configuration. These calculations will also be valuable for optimizing pressure requirements with surface area capacity of the module and performance of the membrane processes as well as isolating other contributions to flow maldistribution.

Acknowledgment

This work was funded by the Australian Research Council through its support of the Commonwealth Special Research Centre for Membrane Science and Technology. V. C. thanks Dr. G. G. Warr and Dr. P. R. Harrowell (Dept. of Physical and Theoretical Chemistry, University of Sydney) for the use of their ball shaking equipment and image analyzer. V. C. also thanks Dr. D. Wiley for useful comments on this article.

Notation

a = cross-sectional area incorporating a fiber (see Eq. 5), m^2
a_f = minimum cross-sectional area for one fiber (1.1207 πr^2 for hexagonal close packing and 1.2732 πr^2 for a square array), m^2
a_i = area of ith size category (Eq. 11), m^2
a_o = average cross-sectional area per fiber (Eq. 5), m^2
A_c = total cross-sectional area in the module available for flow $(A-N\pi r^2)$, m^2
A_{ci} = cross-sectional area in the ith size cell available for flow $(a_i-N\pi r^2)$, m^2
D_h = hydraulic diameter $(4A_c/P_w)$, m
D_{hi} = hydraulic diameter $(4A_c/P_w)$ for the ith cell, m
f = friction factor (Fanning)
fRe = friction factor·Reynolds number
$(fRe)_e$ = effective fRe for fiber bundle
$(fRe)_i$ = fRe for ith size cross-sectional cell (determined by fRe values in order arrays)
L = length of fiber bundle, m
N = total number of fibers
N_i = number of fibers with ith size category
r = radius of fiber, m
Re = Reynold's number $(D_h v\rho/\nu)$
P = probability of fibers within a size range (Eq. 9)
P_i = probability of ith size cross-sectional cell for a fiber
P_w = total wetted perimeter, m
P_{wi} = wetted perimeter for a cell of ith size cross-sectional area, m
Δp = pressure drop, $kg\cdot m^{-1}\cdot s^{-2}$
Q = total fluid flow, $kg\cdot s^{-1}$
Q_i = total fluid flow in the ith cell, $kg\cdot s^{-1}$
v = fluid velocity, $m\cdot s^{-1}$
W_i = fractional flow through channels of the ith category

Greek letters

ϵ = average (bulk) porosity $=(A-N\pi r^2)/A$ $=(1-$packing density)

λ = dimensionless area $(a-a_f)/(a_o-a_f)$
ν = fluid viscosity, $kg \cdot m^{-1} \cdot s^{-1}$
ρ = density, m^3/kg
ϕ = cross-sectional area associated with one fiber (Eq. 4), m^2
$\langle\phi\rangle$ = average (bulk) cross-sectional area per one fiber, m^2

Literature Cited

Alonso, M., M. Satoh, and K. Miyanami, "Void Size Distribution in Two Dimensional Random Packings of Equal Size Disks," *Can. J. Chem. Eng.*, **70**, 28 (1992).

Chan, D. Y. C., B. D. Hughes, and L. Paterson, "Fluid Capacity Distributions of Random Porous Media," *Transport in Porous Media*, **3**, 81 (1988).

Chan, K. L., J. H. F. Lim, and G. A. Davies, "Prediction of the Structure and Blinding of An Inorganic Cellular Membrane in Dead End Filtration," *Int. Technical Conf. on Membrane Separation Processes*, BHRA, Brighton, UK (1990).

Costello, M. J., A. G. Fane, P. A. Hogan, and R. W. Schofield, "The Effect of Shell Side Hydrodynamics on the Performance of Axial Flow Hollow Fiber Modules," *J. Memb. Sci.*, **80**, 1 (1993).

Frenkel, J., *Kinetic Theory of Liquids*, Dover, New York (1955).

Glaser, M. A., and N. A. Clark, "Melting and Liquid Structure in Two Dimensions," *Advances in Chemical Physics*, I. Prigogine and S. A. Rice, eds., Wiley, New York (1993).

Hammer, B. E., C. A. Heath, S. D. Mirer, and G. Belfort, "Quantitative Flow Measurements in Bioreactors by Nuclear Magnetic Resonance Imaging," *Bio/Technol.*, **8**, 327 (1990).

Happel, J., "Viscous Flow Relative to Arrays of Cylinders," *AIChE J.*, **5**, 174 (1959).

Haughey, D. P., and G. S. G. Beveridge, "Local Voidage Variation in a Randomly Packed Bed of Equal-sized Spheres," *Chem. Eng. Sci.*, **21**, 905 (1966).

Haughey, D. P., and G. S. G. Beveridge, "Local Voidage Variations in a Randomly Packed Bed of Equal-sized Spheres," *Chem. Eng. Sci.*, **22**, 715 (1967).

Heath, C. A., G. Belfort, B. E. Hammer, S. D. Mirer, and J. M. Pimbley, "Magnetic Resonance Imaging and Modeling of Flow in Hollow-Fiber Bioreactors," *AIChE J.*, **36**, 547 (1990).

Hinrichsen, Einar, J. Feder, and T. Jossang, "Geometry of Random Sequential Adsorption," *J. Statistical Phys.*, **44**, 793 (1986).

Kuwabra, S., "The Force Experienced by Randomly Distributed Parallel Circular Cylinders or Spheres in a Viscous Flow at Small Reynolds Number," *J. Phys. Soc. Japan*, **14**, 527 (1959).

Meijering, J. L., "Interface Area, Edge Length, and Number of Vertices in Crystal Aggregates with Random Nucleation," *Philips Res. Rep.*, **8**, 270 (1953).

Noda, I., D. G. Brown-West, and C. C. Gryte, "Effect of Flow Maldistribution on Hollow Fiber Dialysis—Experimental Studies," *J. Memb. Sci.*, **8**, 209 (1979).

Rehme, K., "Laminarströmung in Stabbündeln," *Chemie-Ing.-Techn.*, **43**, 962 (1971).

Shah, R. K., and A. L. London, *Laminar Flow Forced Convection in Ducts: A Source Book for Compact Heat Exchanger Analytical Data*, Chapters 15 and 17, Academic Press, New York (1978).

Sparrow, E. M., and A. L. Loeffler, "Longitudinal Laminar Flow Between Cylinders Arranged in Regular Array," *AIChE J.*, **5**, 325 (1959).

Sullivan, R. R., "Specific Surface Measurements on Compact Bundles of Parallel Fibers," *J. Appl. Phys.*, **13**, 725 (1942).

Tomadakis, M. M., and S. V. Sotirchos, "Knudsen Diffusivities and Properties of Structures of Unidirectional Fibers," *AIChE J.*, **37**, 1175 (1991).

Wickramasinghe, S. R., M. J. Semmens, and E. L. Cussler, "Better Hollow Fiber Contactors," *J. Memb. Sci.*, **62**, 371 (1991).

Wickramasinghe, S. R., M. J. Semmens, and E. L. Cussler, "Mass Transfer in Various Hollow Fiber Geometries," *J. Memb. Sci.*, **69**, 235 (1992).

Yang, M.-C., and E. L. Cussler, "Designing Hollow-Fiber Contactors," *AIChE J.*, **32**, 1910 (1986).

Yu, C. P., and T. T. Soong, "A Random Cell Model for Pressure Drop Prediction in Fibrous Filters," *Trans. ASME J. Appl. Mech.*, **E97**, 301 (1975).

Manuscript received Apr. 12, 1993, and revision received July 6, 1993.